

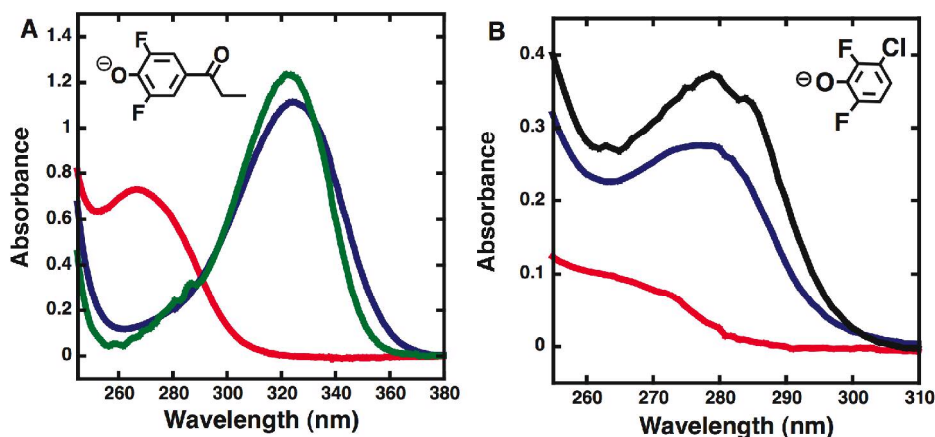
SUPPORTING INFORMATION

Testing Geometrical Discrimination within an Enzyme Active Site: Constrained Hydrogen Bonding in the Ketosteroid Isomerase Oxyanion Hole

Complete Reference 119:

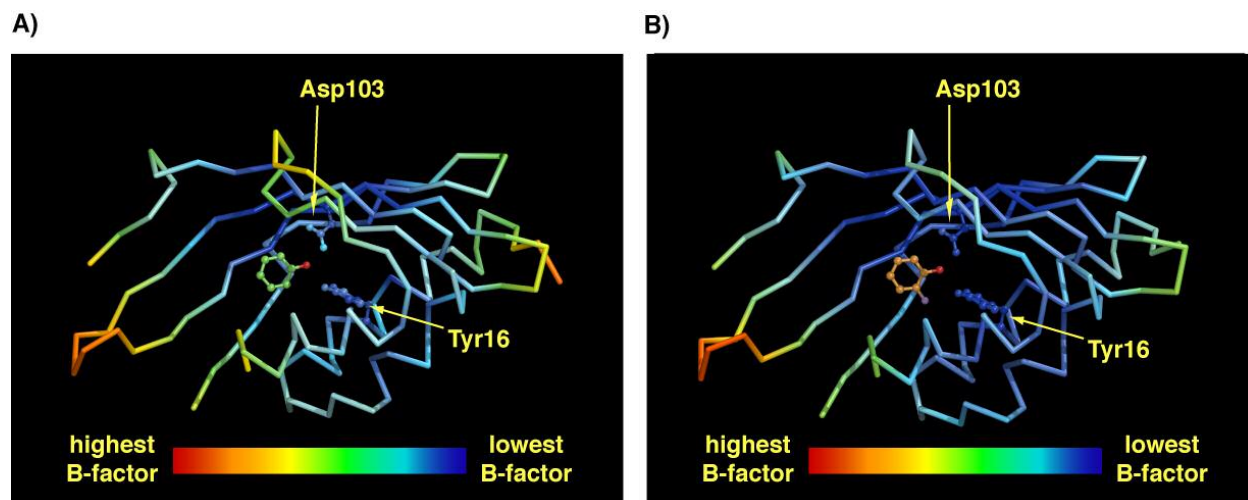
Gaussian 03, Revision C.02, Frisch, M. J.; Trucks, G. W.; Schlegel, H. B.; Scuseria, G. E.; Robb, M. A.; Cheeseman, J. R.; Montgomery, Jr., J. A.; Vreven, T.; Kudin, K. N.; Burant, J. C.; Millam, J. M.; Iyengar, S. S.; Tomasi, J.; Barone, V.; Mennucci, B.; Cossi, M.; Scalmani, G.; Rega, N.; Petersson, G. A.; Nakatsuji, H.; Hada, M.; Ehara, M.; Toyota, K.; Fukuda, R.; Hasegawa, J.; Ishida, M.; Nakajima, T.; Honda, Y.; Kitao, O.; Nakai, H.; Klene, M.; Li, X.; Knox, J. E.; Hratchian, H. P.; Cross, J. B.; Bakken, V.; Adamo, C.; Jaramillo, J.; Gomperts, R.; Stratmann, R. E.; Yazyev, O.; Austin, A. J.; Cammi, R.; Pomelli, C.; Ochterski, J. W.; Ayala, P. Y.; Morokuma, K.; Voth, G. A.; Salvador, P.; Dannenberg, J. J.; Zakrzewski, V. G.; Dapprich, S.; Daniels, A. D.; Strain, M. C.; Farkas, O.; Malick, D. K.; Rabuck, A. D.; Raghavachari, K.; Foresman, J. B.; Ortiz, J. V.; Cui, Q.; Baboul, A. G.; Clifford, S.; Cioslowski, J.; Stefanov, B. B.; Liu, G.; Liashenko, A.; Piskorz, P.; Komaromi, I.; Martin, R. L.; Fox, D. J.; Keith, T.; Al-Laham, M. A.; Peng, C. Y.; Nanayakkara, A.; Challacombe, M.; Gill, P. M. W.; Johnson, B.; Chen, W.; Wong, M. W.; Gonzalez, C.; and Pople, J. A.; Gaussian, Inc., Wallingford CT, **2004**.

Figure S1: Determination of ionization state of di-*ortho*-fluorophenols bound to tKSI^{D40N}.



Absorbance spectra of 50 μM (A) 4-propionyl-2,6-difluorophenol (pK_a 5.4) and (B) 3-chloro-2,6-difluorophenol (pK_a 6.3) measured in 10 mM HCl (red), 10 mM NaOH (blue), and bound to 300 μM tKSI^{D40N} in 40 mM potassium phosphate, pH 7.2 (green), or 10 mM sodium acetate, pH 5.8 (black), were consistent with binding as ionized phenolates. Concentrations of enzyme and phenol were sufficient to give >95% bound phenol (data not shown).

Figure S2: Atomic B-factors for the (A) pKSI^{D40N}•phenolate (PDB code: 2PZV) and (B) pKSI^{D40N}•2-F-phenolate (PDB code: 3CPO) structures.



Backbone colors represent the highest atomic B-factor observed for each residue. D103 and Y16 side-chains also colored according to their atomic B-factors. Ligands (phenolate, green, and 2-F-phenolate, orange) are not colored by B-factors.

Figure S3: Sigma-A weighted $2F_o - F_c$ electron density map of the pKSI^{D40N}•2-F-phenolate oxyanion hole (contoured at 1.3σ).

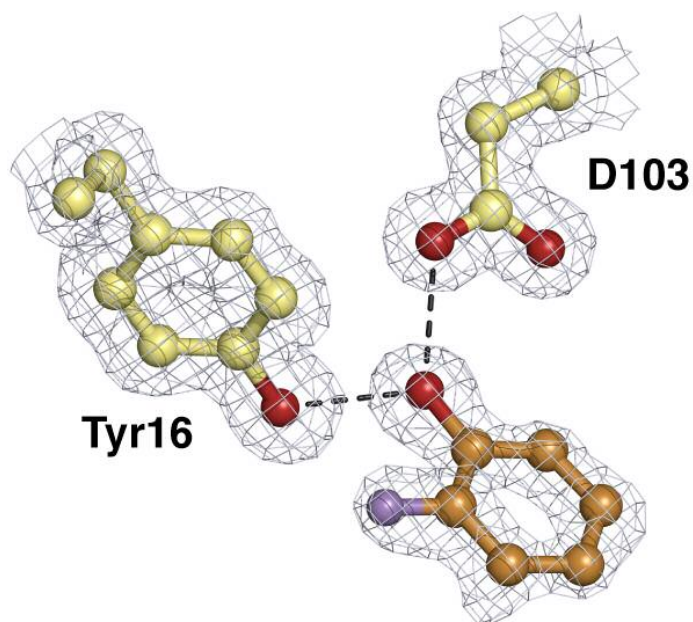
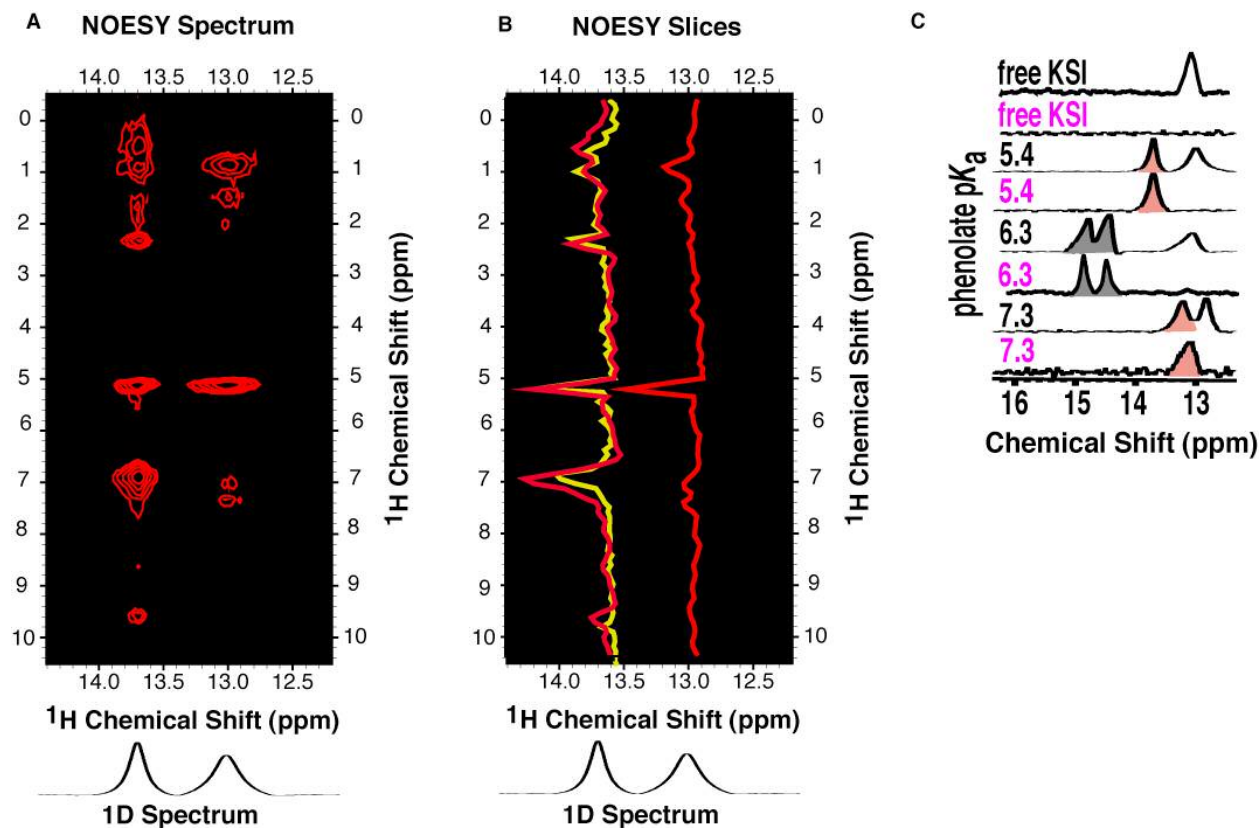


Figure S4: Assignment of the observed downfield peak in $tKSI^{D40N} \bullet DFP$ spectra to an oxyanion hole hydrogen bond.



A H-H NOESY spectrum of $tKSI^{D40N} \bullet 4$ -propionyl-DFP confirmed that NOE cross-peaks formed to the 13.7 ppm downfield peak are distinct from those observed to the 13 ppm peak present in the free enzyme spectrum (A) and are identical to the cross-peaks formed to the most downfield oxyanion hole hydrogen bonded proton peak observed in the previously published $tKSI^{D40N} \bullet 4$ -NO₂-phenolate H-H NOESY spectrum (yellow),¹ as viewed in an overlay of vertical slices from the NOESY spectra (B) and as expected for oxyanion hole hydrogen bonds. Additionally, low pH conditions (5.8), where the 13 ppm enzymatic peak is not detected (violet), had no effect on the appearance or chemical shift of the most downfield peak observed in $tKSI^{D40N} \bullet$ non-ortho-phenolate (black) and $tKSI^{D40N} \bullet DFP$ (red) complexes (C), consistent with assignment of the observed downfield peak to an oxyanion hole hydrogen bond.

Table S1: pKSI^{D40N}•2,6-F₂-phenolate Crystallographic Data-Collection and Refinement Statistics (PDB code: 2INX).

Data Set	
Resolution Range (Å)	47.4-1.50
Space Group	C222 ₁
a, Å	35.1
b, Å	94.9
c, Å	72.4
α, °	90.0
β, °	90.0
γ, °	90.0
Number Unique Reflections	18,650
Completeness	93.7
Multiplicity	9.0
<i>R</i> _{merge} , % ^a	7.9
<i>I</i> / <i>σ</i> _{overall} (<i>I</i> / <i>σ</i> _{high res})	16.1(4.4)
Refinement Statistics	
No. Residues	123
No. Waters	72
<i>R</i> _{work} , % ^b	18.5
<i>R</i> _{free} , % ^c	23.4
rmsd bond, Å	0.021
rmsd angle, °	1.9
^a $R_{merge} = \frac{\sum_{hkl} \sum_i I(hkl)_i - \{I(hkl)\} }{\sum_{hkl} \sum_i I(hkl)_i}$ ^b $R_{work} = \frac{\sum_{hkl} F(hkl)_o - \{F(hkl)_c\} }{\sum_{hkl} F(hkl)_o}$ ^c <i>R</i> _{free} was calculated exactly as <i>R</i> _{work} where F(hkl) _o were taken from 10% of the data not included in refinement.	

Table S2: pKSI^{D40N}•2-F-phenolate Crystallographic Data Collection and Refinement Statistics (PDB code: 3CPO).

Data Set	
Resolution Range (Å)	50-1.24
Space Group	C222 ₁
a, Å	35.3
b, Å	95.0
c, Å	72.4
α, °	90.0
β, °	90.0
γ, °	90.0
Number Unique Reflections	33,296
Completeness	95.3
Multiplicity	11.3
R_{merge} , % ^a	5.3
$I/\sigma_{overall}$ ($I/\sigma_{high\ res}$)	14.7(2.0)
Refinement Statistics	
No. Residues	123
No. Waters	71
R_{work} , % ^b	16.6
R_{free} , % ^c	20.0
rmsd bond, Å	0.022
rmsd angle, °	1.95
^a $R_{merge} = \frac{\sum_{hkl} \sum_i I(hkl)_i - \{I(hkl)\} }{\sum_{hkl} \sum_i I(hkl)_i}$ ^b $R_{work} = \frac{\sum_{hkl} F(hkl)_o - \{F(hkl)_c\} }{\sum_{hkl} F(hkl)_o}$ ^c R_{free} was calculated exactly as R_{work} where $F(hkl)_o$ were taken from 5% of the data not included in refinement.	

Table S3: NMR chemical shift of downfield peak in tKSI^{D40N}•di-ortho-fluorophenolate complexes.

Phenolate	pK _a ^a	δ _{ppm}
4-propionyl-2,6-F ₂	5.4	13.7
2,3,5,6-F ₄	5.7	13.6
F ₅	5.7	14.0
3-Cl-2,6-F ₂	6.3	14.0
2,3,6-F ₃	6.5	14.0
2,4,6-F ₃	7.2	13.4
3-Me-2,6-F ₂	7.3	13.2

^a Determined by spectral titration, as previously described.¹

Table S4: NMR chemical shift of hydrogen-bonded proton detected in small molecule complexes.

Phenol (pK_a)	Chemical Shift (ppm)	
	4-nitropyridine-N-oxide ($pK_a = -1.7$) ²	2,6-dichloropyridine-N-oxide ($pK_a = -2.3$) ³
3,4-dinitrophenol (5.4) ²	11.4	11.1
3-CF ₃ -4-nitrophenol (6.3) ¹	10.7	10.6
4-nitrophenol (7.1) ²	10.0	10.0
4-cyanophenol (8.0) ²	9.4	9.5

Table S5: Affinities of di-*ortho*-fluorophenolates for KSI^{D40N} determined by fluorescence binding.

Phenolate	pK_a^a	pKSI ^{D40N}		tKSI ^{D40N}	
		K_d^{app} (μM) ^b	K_d (μM) ^b	K_d^{app} (μM) ^b	K_d (μM) ^b
2,3,5,6-F ₄	5.7	142 (53)	0.41 (0.15)	320 (6)	0.91 (0.02)
F ₅	5.7	108 (23)	0.31 (0.07)	280 (6)	0.79 (0.02)
2,3,6-F ₃	6.5	188 (17)	0.53 (0.05)	630 (150)	1.76 (0.41)
2,6-F ₂	7.1	633 (179)	1.62 (0.46)	1770 (580)	4.53 (1.48)
2,4,6-F ₃	7.2	530 (94)	1.34 (0.24)	2540 (1540)	6.41 (3.88)

^a Determined by spectral titration, as previously described.¹

^b K_d^{app} is defined as the apparent affinity at pH 8. K_d is defined as the pH-independent affinity. Errors (in parenthesis) are average deviations

References:

- (1) Kraut, D. A.; Sigala, P. A.; Pybus, B.; Liu, C. W.; Ringe, D.; Petsko, G. A.; Herschlag, D. *PLoS Biol.* **2006**, *4*, e99.
- (2) Jencks, W. P.; Regenstein, J. In *Handbooks of Biochemistry and Molecular Biology*; Fasman, G. D., Ed.; CRC Press: Cleveland, 1976, p 305-351.
- (3) Johnson, C. D.; Katritzky, A. R.; Shakir, N. *J. Chem. Soc. B* **1967**, 1235-1237.